



ARTICLE

<https://doi.org/10.1038/s42004-019-0118-3>

OPEN

# Natural ligand-nonmimetic inhibitors of the lipid-transfer protein CERT

Naoki Nakao<sup>1</sup>, Masaharu Ueno <sup>2,4</sup>, Shota Sakai<sup>3</sup>, Daichi Egawa<sup>3</sup>, Hiroyuki Hanzawa<sup>1</sup>, Shohei Kawasaki<sup>1</sup>, Keigo Kumagai<sup>3</sup>, Makoto Suzuki<sup>1</sup>, Shu Kobayashi <sup>2</sup> & Kentaro Hanada <sup>3</sup>

Lipid transfer proteins mediate inter-organelle transport of membrane lipids at organelle contact sites in cells, playing fundamental roles in the lipidome and membrane biogenesis in eukaryotes. We previously developed a ceramide-mimetic compound as a potent inhibitor of the ceramide transport protein CERT. Here we develop CERT inhibitors with structures unrelated to ceramide. To this aim, we identify a seed compound with no ceramide-like structure but with the capability of forming a hydrogen-bonding network in the ceramide-binding START domain, by virtual screening of  $\sim 3 \times 10^6$  compounds. We also establish a surface plasmon resonance-based system to directly determine the affinity of compounds for the START domain. Then, we subject the seed compound to a series of *in silico* docking simulations, efficient chemical synthesis, affinity analysis, protein-ligand co-crystallography, and various *in vivo* assays. This strategy allows us to obtain ceramide-unrelated compounds that potently inhibited the function of CERT in human cultured cells.

<sup>1</sup>Structure-Based Drug Design Group, Organic Synthesis Department, Daiichi Sankyo RD Novare Co. Ltd., 1-16-13 Kitakasai, Edogawa-ku, Tokyo 134-8630, Japan. <sup>2</sup>Department of Chemistry, School of Science, the University of Tokyo, Hongo, Bunkyo-ku, Tokyo 110-0033, Japan. <sup>3</sup>Department of Biochemistry & Cell Biology, National Institute of Infectious Diseases, 1-23-1 Toyama, Shinjuku-ku, Tokyo 162-8640, Japan. <sup>4</sup>Present address: Department of Natural Science, Graduate School of Advanced Technology and Science, Tokushima University, 2-1 Minami-jousanjima, Tokushima 770-8506, Japan. These authors contributed equally: Naoki Nakao, Masaharu Ueno, Shota Sakai. Correspondence and requests for materials should be addressed to S.K. (email: [shu\\_kobayashi@chem.s.u-tokyo.ac.jp](mailto:shu_kobayashi@chem.s.u-tokyo.ac.jp)) or to K.H. (email: [hanak@nih.go.jp](mailto:hanak@nih.go.jp))

Lipids are the major constituents of all cell membranes and play dynamic roles in organelle structure and function. In eukaryotes, the endoplasmic reticulum (ER) is the main center for the synthesis of diverse lipid types in cells, and lipids newly synthesized in the ER are delivered to other organelles by a variety of lipid-transfer proteins (LTPs), which mediate inter-organelle transport at organelle membrane contact sites in a nonvesicular manner<sup>1–3</sup>. Thus, LTPs play fundamental roles in the regulation of the lipidome and membrane biogenesis in cells. Moreover, several LTPs have roles beyond that of an inter-membrane lipid carrier. For example, an oxysterol-binding protein not only mediates sterol transfer from the ER to the Golgi apparatus but also functions as a cholesterol-dependent scaffolding protein in the extracellular signal-regulated kinase pathway<sup>4,5</sup>. Hence, LTPs have been rapidly gaining attention as a novel type of molecular medicinal target. Nevertheless, specific inhibitors of LTPs are limited.

The ceramide transport protein CERT, a typical LTP, mediates the transport of ceramide from the ER to the Golgi apparatus, in which ceramide is converted to the phosphosphingolipid sphingomyelin (SM)<sup>6,7</sup>. CERT has several advantages as a model LTP for the development of novel inhibitors with a rational strategy. First, various assay systems to analyze the activities of CERT and its functional modules have been established<sup>6</sup>. Second, the physiological roles of CERT in various organisms from cultured cells to model animals (e.g., fruit fly, zebrafish, and mouse) have been elucidated<sup>6,8–10</sup>. Of note, a point mutation that renders CERT to be constitutively active is the causative mutation responsible for a human hereditary mental development disorder with an autosomal dominant inheritance<sup>11</sup>. Thus, CERT was demonstrated to be a key player in the homeostasis of the ceramide–SM axis of the cellular lipidome, and it follows that its dysregulation leads to pathological outcomes. Additionally, co-crystallography of the ceramide-binding START domain of CERT with multiple types of ceramide species was resolved<sup>12</sup>. Moreover, a potent inhibitor of CERT named (1R, 3S)-HPA-12, which contains a ceramide-like moiety, was previously developed and characterized<sup>13–17</sup>. Although several derivatives of ceramides and HPA-12 were shown to have enhanced binding affinity for the CERT START domain under cell-free conditions<sup>18–20</sup>, it is not known whether these new derivatives are capable of inhibiting CERT in living cells more potently than the original HPA-12. HPA-12 binds to the ceramide-binding pocket in the CERT START domain, thereby acting as a competitive antagonist, whereas it does not affect the ceramide-metabolizing enzymes, including ceramide synthase, SM synthase, ceramidase, and sphingomyelinase. Nevertheless, HPA-12 might serve as a direct ligand for one or more yet-to-be determined proteins that recognize ceramides. Similar concerns inevitably accompany artificial compounds having structural mimicry to a natural ligand. Namely, natural ligand-mimetic compounds may directly bind to not only the desired target but also to various undesired targets sharing the same natural ligand.

Herein, we describe the development of a series of small chemicals with no apparent ceramide mimicry, but with potent activity to inhibit the function of CERT in human cultured cells. The establishment of the ligand-mimetic and nonmimetic inhibitor sets of CERT may provide a pharmacological tool to discriminate on-target effects from off-target effects when CERT is pharmacologically inhibited as the same pathophysiological consequences induced by a pair of structurally dissimilar inhibitors are attributable directly or indirectly to the inhibition of CERT, not to off-target effects.

## Results

**Physical affinity of compounds for CERT.** To determine the physical affinity of low-molecular-weight chemicals for CERT, we developed a quantitative assay system in which purified recombinant CERT START domain was immobilized on a surface plasmon resonance (SPR) sensor, and then the system was validated using the known CERT inhibitor HPA-12. After analyzing the affinity of four stereoisomers of HPA-12 for the CERT START domain, the  $K_d$  values of the (1R, 3S)-, (1S, 3R)-, (1S, 3S)-, and (1R, 3R)-isomers were estimated to be ~30, >10,000, ~4500, and ~4000 nM, respectively (Fig. 1a, b and Supplementary Fig. 1). These  $K_d$  values were almost identical to those obtained for the full-size CERT (Fig. 1b and Supplementary Fig. 1). These results were qualitatively consistent with previous studies using living cells<sup>13,16</sup> and indirect competitive cell-free assays<sup>21</sup>, although smaller differences in the binding activities among the HPA stereoisomers were reported in the indirect competitive assay systems<sup>21</sup>. The newly developed assay system enabled us to determine the  $K_d$  values of short-chain  $C_4$ -ceramide ( $K_d = 93$  nM) and  $C_6$ -ceramide ( $K_d = 58$  nM) for CERT (Supplementary Fig. 1), showing that a hydrophobic interaction between the acyl chain of ceramides and the ligand-recognition pocket of the START domain contributes to the ligand affinity in line with a previous study on co-crystals of the START domain in complex with various ceramide species<sup>12</sup>. The affinity for the long-chain  $C_{16}$ -ceramide could not be tested because of its poor water miscibility. Collectively, we concluded that the SPR assay system may be useful to accurately determine the  $K_d$  values of small compounds for the CERT START domain.

**Virtual screening of ceramide-unlike compounds for CERT.** To identify seed compounds that were not structurally similar to ceramide, we exploited previously solved three-dimensional (3D) structures of the CERT START domain in complex with natural ceramides and ceramide-mimetic inhibitors for protein–chemical compound docking-based in silico screening (Supplementary Fig. 3). After virtual screening of  $\sim 3 \times 10^6$  compounds, we found one candidate hereafter referred to as seed compound 1 (SC1), which has no apparent ceramide-like structure (Fig. 1c). The SPR assay demonstrated that SC1 bound to the CERT START domain with a  $K_d$  value of  $\sim 12$   $\mu$ M (Fig. 1c). Moreover, X-ray crystallography analysis confirmed the predicted hydrogen-bonding network between SC1 and the ceramide-binding pocket in the co-crystal complex (Fig. 1d and Supplementary Fig. 3). Based on these results, we determined SC1 was a promising initial compound for the development of a natural ligand-nonmimetic inhibitor of CERT.

**Various derivative series of SC1.** For the systematic expansion of SC1 derivatives, the structural backbone of the seed compound needed to be simple but adaptable to combinatorial synthesis. Thus, we examined the dispensability of the fluorine, methyl, and azole groups of SC1 to interact with the CERT START domain. Elimination of the fluorine or methyl group or both together did not reduce the affinity for CERT (Supplementary Fig. 2). Importantly, changing the azole moiety to  $C\equiv C$ ,  $C-C$ , *cis*  $C=C$ , *trans*  $C=C$ , or racemic cyclopropyl groups did not abrogate the interaction with CERT, although none of these groups substantially increased the affinity compared with the azole group (Supplementary Fig. 2). Thus, we decided to simplify the azole moiety to these five groups for the construction of chemical derivative panels. The five series of compounds having a  $C\equiv C$ ,  $C-C$ , *cis*  $C=C$ , *trans*  $C=C$ , or *cis* cyclopropyl group in place of the azole were referred to as the A, B, C, D, and E series, respectively (Supplementary Fig. 2). Then, the various compounds of these

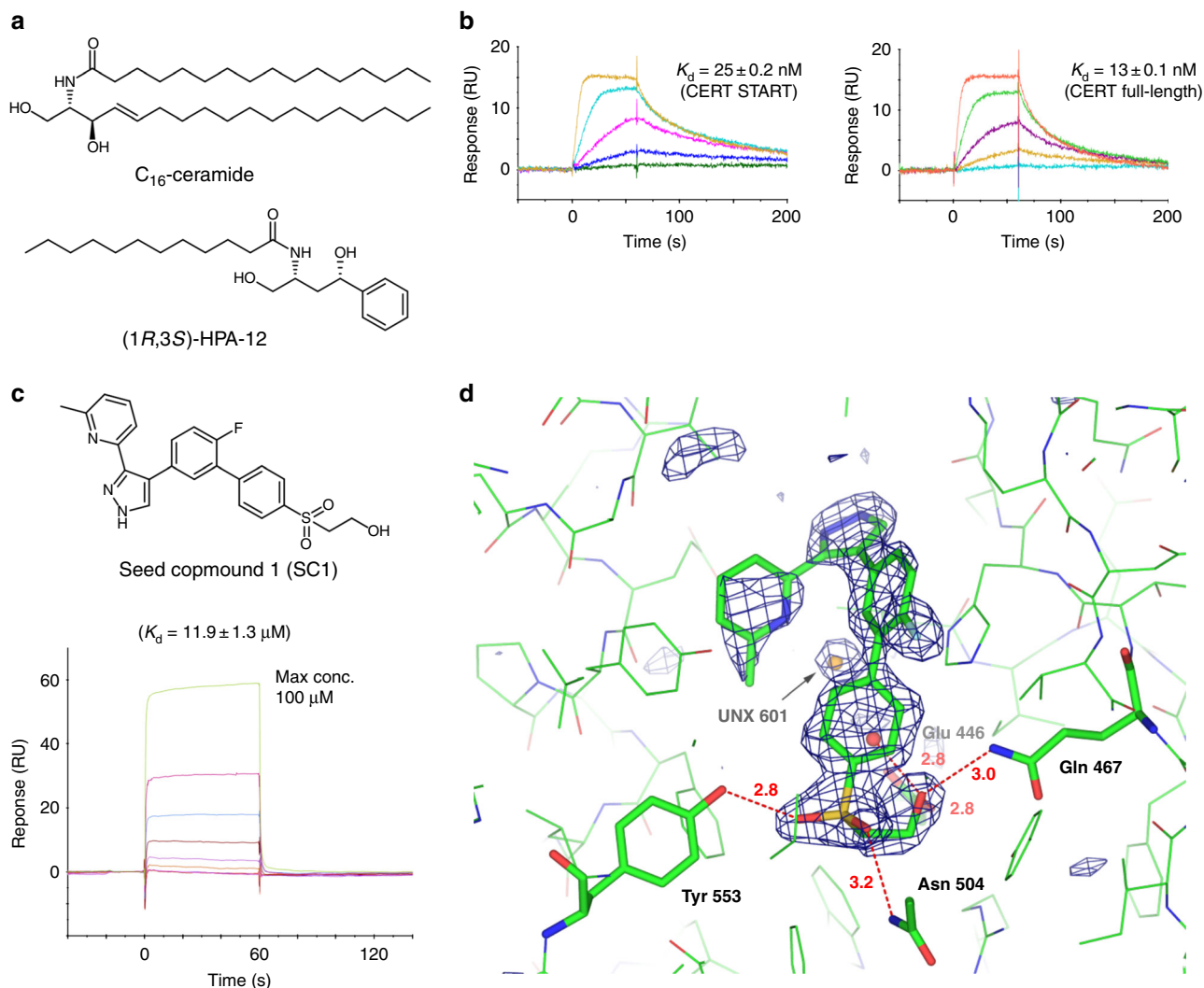


**Fig. 1** Virtual screening of ceramide-nonmimetic inhibitors of CERT. **a** Structure of  $C_{16}$ -ceramide, (1R, 3S)-HPA-12. **b** Affinities of (1R, 3S)-HPA-12 for the full-size CERT and CERT START domain immobilized on an SPR sensor chip were determined. The  $K_d$  values were obtained by kinetics fitting of the SPR data. **c** Seed compound 1 (SC1) for novel CERT inhibitors without ceramide-like structures. An SPR sensor gram of the immobilized CERT START domain at various concentrations of SC1 as the analyte is shown. The  $K_d$  value was determined by the affinity-fitting method because it could not be determined by the kinetics fitting. **d** Capturing of SC1 by CERT. Co-crystallography of the CERT START domain in complex with SC1 is shown. Red dashed lines, hydrogen bonds (distances are indicated in angstroms); red balls, water molecules. Residual electron density is represented as UNX (unknown atom or ion)

five series were synthesized (Supplementary METHODS, and Supplementary Figs. 10–32), and analyzed for their affinity toward the CERT START domain. Notably, we used a one-pot tandem reaction system for efficient chemical synthesis of the A-series compounds except for A15 (Supplementary METHODS).

When fluorine or methyl or both were added to these five series in the same manner as the initial seed compound SC1, the affinity for CERT tended to be slightly improved in all five series (Fig. 2 and Supplementary Fig. 2). Among them, E3 exhibited the best affinity ( $K_d = 5.6 \mu\text{M}$ ). The co-crystal structure of the CERT START domain with SC1 showed considerable space at the 3-position of the second aromatic moiety (Fig. 1d and Supplementary Fig. 2). The addition of a *tert*-butyl group to the 3-position clearly enhanced the CERT affinity in the B and E series (the derivatives are named B5 and E5, respectively), while it somewhat abrogated the affinity in the other three series (Fig. 2 and Supplementary Fig. 2). Co-crystal analysis revealed that the additional *tert*-butyl group in B5 and E5 did not affect the hydrogen-bonding pattern of the hydroxyethanesulfonyl group, but unexpectedly caused the reorientation of the distal aromatic

group (Fig. 3). This reorientation enabled B5 and E5 to occupy the hydrophobic pocket in a more “ceramide-like” manner compared with SC1 (Fig. 3 and Supplementary Fig. 3).

#### High-affinity CERT inhibitors with no ceramide-like moiety.

We synthesized more derivatives in the A–E series, and eventually identified an encouraging compound named E14 with a  $K_d = \sim 0.7 \mu\text{M}$  for the CERT START domain (Fig. 2). E14 has an *n*-propyl group at the 4-position of the 1,1'-biphenyl moiety (Fig. 4a). We subjected E14 and other compounds to metabolic lipid-labeling experiments to determine their effect on the function of CERT in human cervical cancer-derived HeLa cells (Fig. 4b). At  $1 \mu\text{M}$ , E14 inhibited the labeling of SM by  $\sim 50\%$  while it did not affect the metabolic labeling of glycosphingolipids, phosphatidylserine or phosphatidylethanolamine, all of which are synthesized by CERT-independent pathways. The prototype of the E series (E1) with no alkyl group at the 4-position of the 1,1'-biphenyl moiety did not inhibit the synthesis of SM in line with its undetectable affinity for the CERT START domain (Fig. 2 and Supplementary Fig. 2).

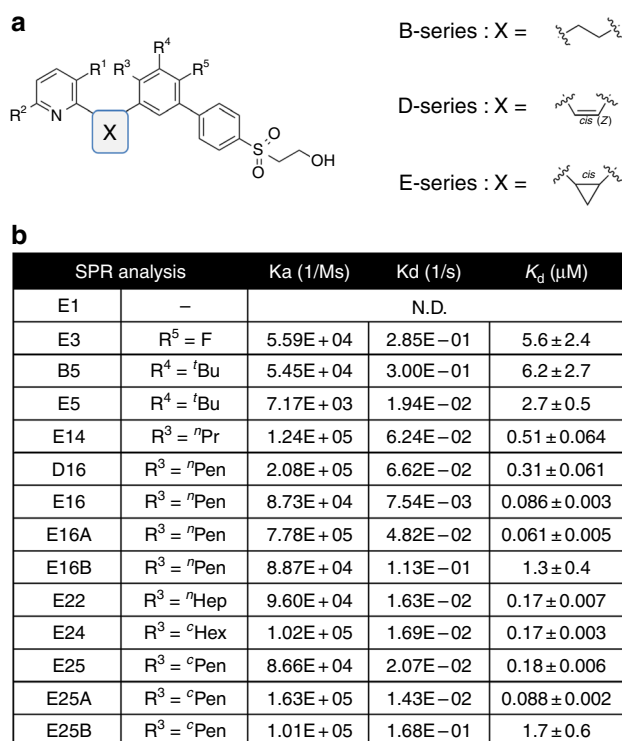


**Fig. 2** Compounds with various levels of affinity for the CERT START domain. **a** Chemical structures of compounds. **b** Affinity for the CERT START domain. The affinity of compounds for the CERT START domain immobilized on SPR sensor chips were analyzed. The  $K_d$  values (the mean values ± SD from three experiments) were determined by kinetics fitting. Both  $R^1$  and  $R^2$  in these compounds are hydrogens. Note that the E-series compounds are racemic at the *cis* cyclopropyl linker. N.D., not determined

X-ray crystallography revealed an empty space at the end of the *n*-propyl group of E14 in the complex with the CERT START domain (Fig. 4c). Thus, we designed new derivatives to better fit the space and found various compounds with high affinity for the CERT START domain *in vitro* (Fig. 2) and with the capability to effectively inhibit the function of CERT in cells (Fig. 4b). Among them, E16 and E25, the two compounds exhibiting the highest affinity ( $K_d$ , ~90 nM for E16 and ~180 nM for E25) for the START domain, were further examined by X-ray crystallography. In the co-crystals, the two compounds were accommodated in the ceramide-binding pocket of the START domain with essentially the same orientation pattern as described for E5 and E14: the hydroxyethanesulfonyl group formed a hydrogen-bonding network, while the hydrophobic moieties occupied the hydrophobic interior of the pocket (Figs 3, 4c, and Supplementary Fig. 4). The alkyl group at the 4-position of the 1,1'-biphenyl moiety of the E compounds was extended to a space where the *N*-acyl moiety of ceramide occupies in the complex with natural ceramide, while the distal aromatic group of the E compounds was extended to a space where the sphingoid base moiety occupies in the ceramide complex (Figs 3, 4c, and Supplementary Figs. 3 and 4). Although E14, E16, and E25 are racemic at the cyclopropane-linker part, only one enantiomer ((1*S*, 2*R*)-isomer) was detected in the co-crystals (Fig. 4c, and Supplementary Fig. 4), suggesting this specific enantiomer has higher CERT affinity. In the co-crystal, there was an empty space beyond the distal end of the pentyl group at the 4-position in E16 (Supplementary Fig. 4c). However, longer alkyl groups at the same position (E22–25) did not improve the affinity for the START domain (Fig. 2). These results

suggested that *n*-pentyl group was nearly the optimal alkyl length at the 4-position.

**Separated enantiomers of E16 and E25.** Compounds of the E series were mixtures of the *cis*-racemate at the cyclopropyl-linker moiety. Both enantiomers of E16 and E25 could be separated by high-performance liquid chromatography (HPLC) with a chiral oligosaccharide-conjugated silica gel. The separated isoforms were tentatively referred to as E16A, E16B, E25A, and E25B, in which the A- and B-types represented the isomers with faster and slower mobilities in the HPLC, respectively (Supplementary Fig. 33). X-ray crystallography of the separated enantiomers in complex with the CERT START domain showed that the A-type has the (1*S*, 2*R*)-configuration at the cyclopropyl linker in E16 and E25 (Fig. 5b, c). Additionally, the (1*R*, 2*S*)-configuration of E25B was confirmed by co-crystallography (Fig. 5d), while we failed to obtain a co-crystal with E16B suitable for X-ray diffraction analysis. From SPR analysis, the  $K_d$  values of E16A, E16B, E25A, and E25B for the CERT START domain were determined to 61, 1300, 88, and 1700 nM, respectively (Figs 2, 5a). The higher affinity of the A-type compounds compared with their B-type counterparts was consistent with the fact that only the A-type was observed in the co-crystals of the CERT START domain prepared with the racemic E series compounds (Figs 3, 4c, and Supplementary Fig. 4). Additionally, the distal pyridine ring of E25B was disordered in the co-crystal compared with the ring of E25A (Fig. 5c, d), explaining the lower affinity of the B-type compounds. B16 and D16 bound to the CERT START domain with essentially the same stereochemical conformation as E16A (Fig. 5b and Supplementary Fig. 4).

#### (1*S*, 2*R*)-HPCB-5, a ceramide-nonmimetic inhibitor of CERT.

The E16 and E25 enantiomers were analyzed in various bioassays. None of these compounds affected the growth of HeLa cells in the normal culture medium containing 10% serum up to 10  $\mu$ M (Fig. 6a). In line with their  $K_d$  values for CERT, the A-types of E16 and E25 were found to be more potent inhibitors than their B-type counterparts: the  $IC_{50}$  values of E16A and E25A in the presence of 10% serum were 0.18 and 0.25  $\mu$ M, respectively, while those of E16B and E25B were 0.76 and 1.93  $\mu$ M, respectively (Fig. 6b). The  $IC_{50}$  values of the most active isomer HPA-12, (1*R*, 3*S*)-HPA-12, and its enantiomer (1*S*, 3*R*)-HPA-12 were 0.2 and >3  $\mu$ M, respectively (Fig. 6b). These results indicated that E16A acts as a highly potent CERT inhibitor in cultured cells similar to (1*R*, 3*S*)-HPA-12. Between the enantiomers E16A and B, there was only an approximately fourfold difference in the  $IC_{50}$  values (0.18 vs. 0.76  $\mu$ M) for the inhibition of SM synthesis in living cells whereas a ~20-fold difference in the  $K_d$  values (61 vs. 1300 nM) in the cell-free SPR assay was observed. Although the reasons for this quantitative inconsistency are not clear, in cultured cells E16A and B might be slightly different in their stability, membrane permeability, and/or protein binding among other factors.

We next examined possible off-target effects. Brefeldin A (BFA) is a pharmacological tool used to merge the Golgi apparatus with the ER. In cells treated with BFA, the conversion of ceramide to SM occurs in the ER/Golgi merged structure in a CERT-independent manner<sup>13,22</sup>. (1*R*, 3*S*)-HPA-12 or the E-series compounds (E16A, E16B, E25A, and E25B) did not affect the synthesis of SM in BFA-treated HeLa cells (Fig. 6c), eliminating the possibility that E16A directly inhibited SM synthases. Myriocin/ISP-1, a specific inhibitor of serine palmitoyltransferase<sup>23</sup>, clearly inhibited the metabolic labeling of SM regardless of BFA (Fig. 6c), ruling out the possibility that BFA treatment non-specifically rendered the cells tolerant to sphingolipid inhibitors.



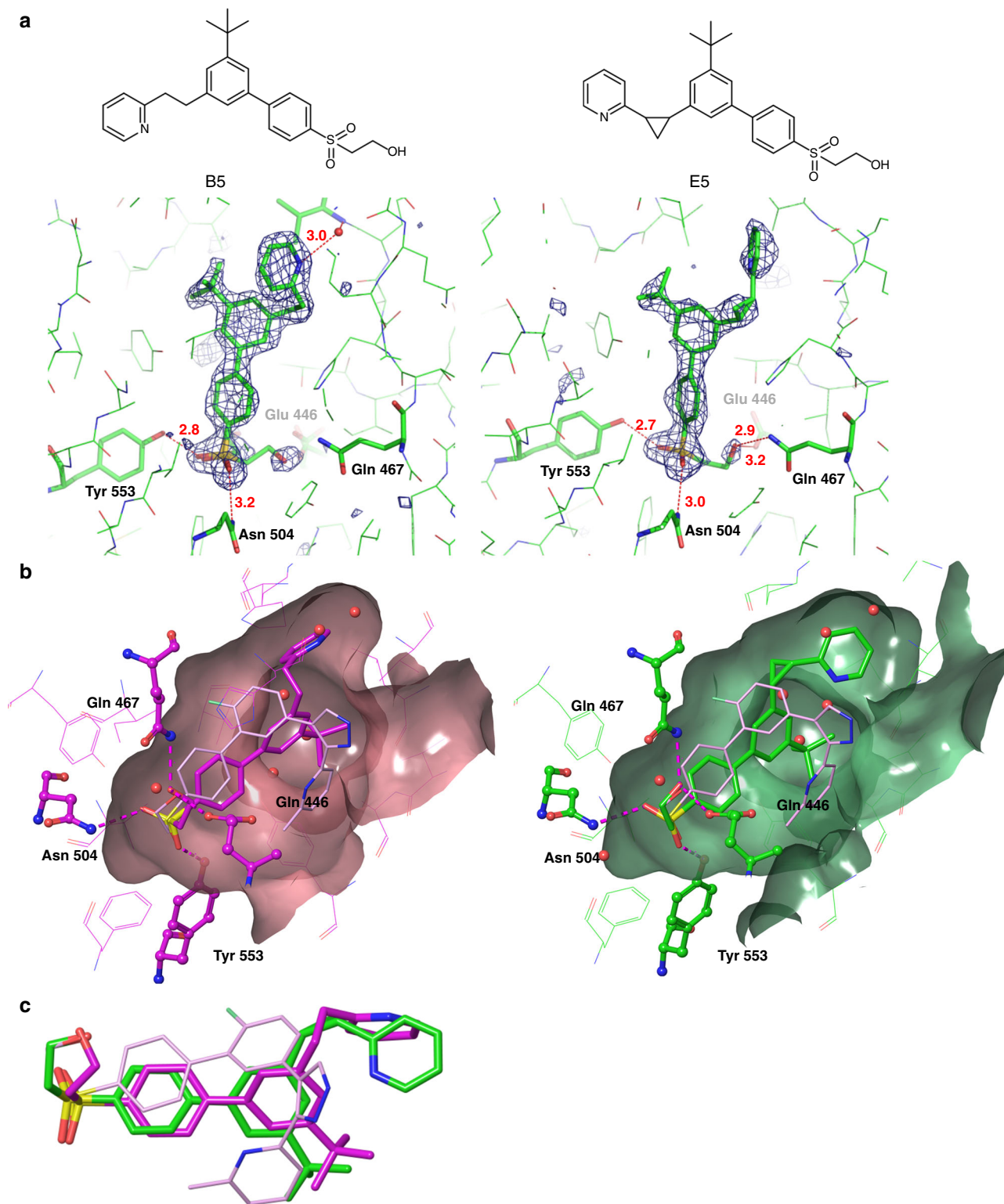


**Fig. 3** X-ray crystallography of the CERT START domain in complex with B5 and E5. **a** Co-crystal images of the CERT START domain in complex with B5 and E5 are shown. Red dashed lines: hydrogen bonds (distances are indicated in angstrom). Blue meshes indicate electron density of the bound compound contoured at 3sigma. **b** Overlaid images of B5 (represented as magenta, left of panel) and E5 (represented as green, right of panel) with SC1 (represented as pink) bound to the CERT START domain. **c** Overlaid images of B5 (magenta), E5 (green), and SC1 (pink) bound to the CERT START domain

We also examined the effects of CERT inhibitors on the lipidome of cells. For lipidome analysis, we used a serum-free medium for cell culture because the use of a metabolic inhibitor to reduce the amount of certain types of cellular sphingolipids may be compensated by serum-derived sphingolipids<sup>24</sup>. When HeLa

cells were cultured in the presence of the inhibitors for 3 days, (1*R*, 3*S*)-HPA-12, E16A, and E25A reduced the amount of SM to ~40% of the drug-untreated control level, while the amounts of other lipid types were not significantly affected (Fig. 6d and Supplementary Figs. 6 and 7).

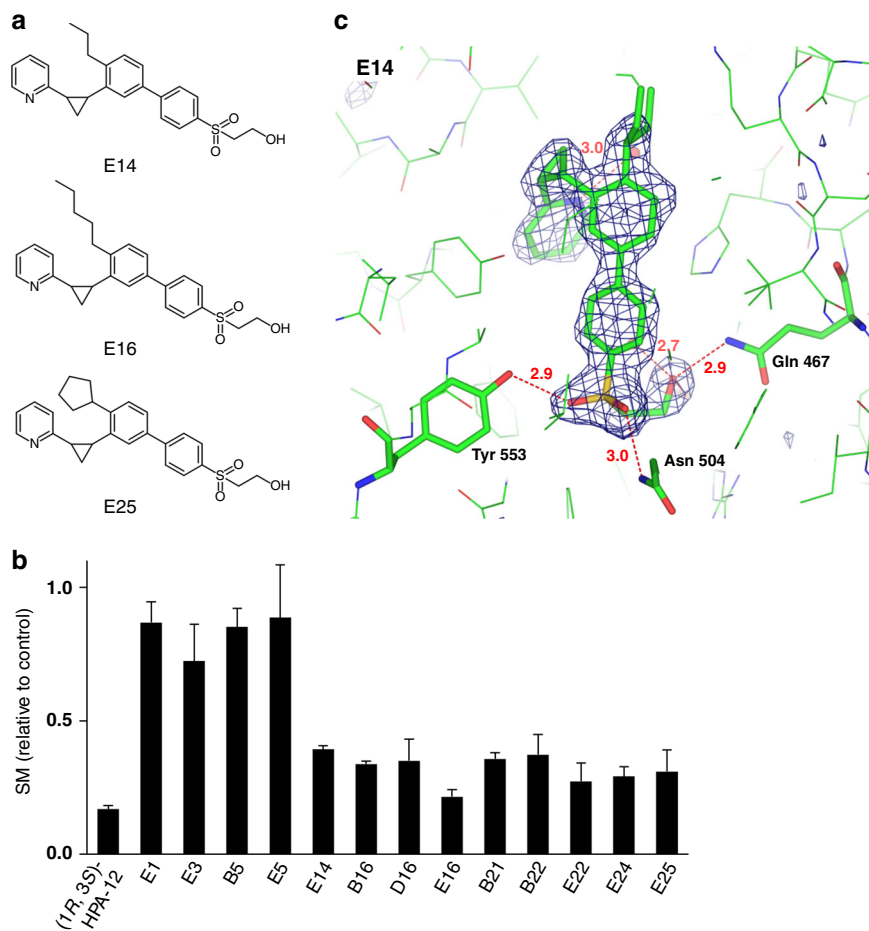


**Fig. 4** Ceramide-nonmimetic inhibitors of CERT are effective in living cells. **a** Structures of novel compounds capable of potentially inhibiting CERT. **b** Inhibition of the function of CERT in HeLa cells by various compounds. HeLa cells were cultured in serum-free medium with the indicated compounds at 1  $\mu$ M (or the vehicle DMSO for the non-treated control) and in the presence of radioactive serine for 24 h. Then, the levels of labeled lipids per protein were determined. Data are shown as the relative values of the vehicle control. The mean values  $\pm$  SD from three experiments are shown. **c** Co-crystallography of the CERT START domain in complex with E14 is shown. Note that although E14 is racemic at the *cis* cyclopropyl linker, co-crystals with the (1*S*, 2*R*)-enantiomer were predominantly obtained (see also text)

Mammalian cells have at least two pathways to deliver ceramide from the ER to the Golgi for the synthesis of SM<sup>6,22,25</sup>. One is the CERT-dependent nonvesicular pathway, and another is a yet-to-be elucidated CERT-independent pathway. Thus, CERT-deficient cells still exhibit a low but detectable capability of *de novo* synthesis of SM<sup>6,22,25</sup>. Whereas (1*R*, 3*S*)-HPA-12, E16A, and E25A reduced the metabolic labeling of SM to  $\sim$ 10% of the non-treated control in wild-type HeLa cells, they did not affect the labeling of SM in CERT-disrupted HeLa cells (Fig. 6e and Supplementary Fig. 5), indicating that the compounds inhibit the CERT-dependent synthesis of SM, but not CERT-independent synthesis.

The miscibility of CERT inhibitors in culture medium was checked by turbidimetric analysis. Neither discernible turbidity was induced by 30  $\mu$ M E16A, B16, nor HPA-12 (Supplementary Fig. 8), suggesting that these CERT inhibitors were soluble up to at least 30  $\mu$ M in the normal culture medium. We next compared the stability of these CERT inhibitors in the culture medium. When these compounds were incubated in the cell-free culture medium containing 10% serum at 37  $^{\circ}$ C, they exhibited no appreciable loss up to at least 72 h as shown by quantitative mass spectrometry analysis (Supplementary Fig. 9a). To analyze the stability of the compounds co-cultured with living cells, E16A, B16, and HPA-12 were added to HeLa cells at 3  $\mu$ M and

cultivated for various time periods. Then the levels of the CERT inhibitors retrieved from the medium were quantified. The levels of E16A, B16, and HPA-12 retrieved from the culture medium slowly decreased throughout 72 h (Supplementary Fig. 9b), suggesting gradual degradation of the inhibitors in the cell culture. This is in agreement with a recent study showing *in vivo* degradation of fluorinated HPA-12 in mice<sup>26</sup>. The cell-associated levels of these compounds reached peaks during the initial 4 h, partially decreased, and then plateaued up to 72 h (Supplementary Fig. 9c). Interestingly, the plateau levels of E16A and B16 were three- to fourfold higher than the level of HPA-12 (Supplementary Fig. 9c). Although the actual reason for this difference is unknown, HPA-12 might be more favorably trapped by serum proteins (e.g., albumin and lipoproteins), or more preferentially exported from cells (e.g., via multidrug ABC transporters), compared with E16A and B16. These results suggest that E16A and B16 exert slightly more prolonged activity than HPA-12 in cell culture.

We hereafter renamed E16A to (1*S*, 2*R*)-HPCB-5, or abbreviated it to HPCB-5 after its chemical name of 4'-(2-hydroxyethanesulfonyl)-4-pentyl-3-(2-(pyridin-2-yl)-(1*S*, 2*R*)-cyclopropyl)-1,1'-biphenyl (the 5 of HPCB-5 represents the C5 pentyl group). Although B16 was slightly less active as a CERT inhibitor than E16 (Fig. 4b), the fact that B16 does not contain

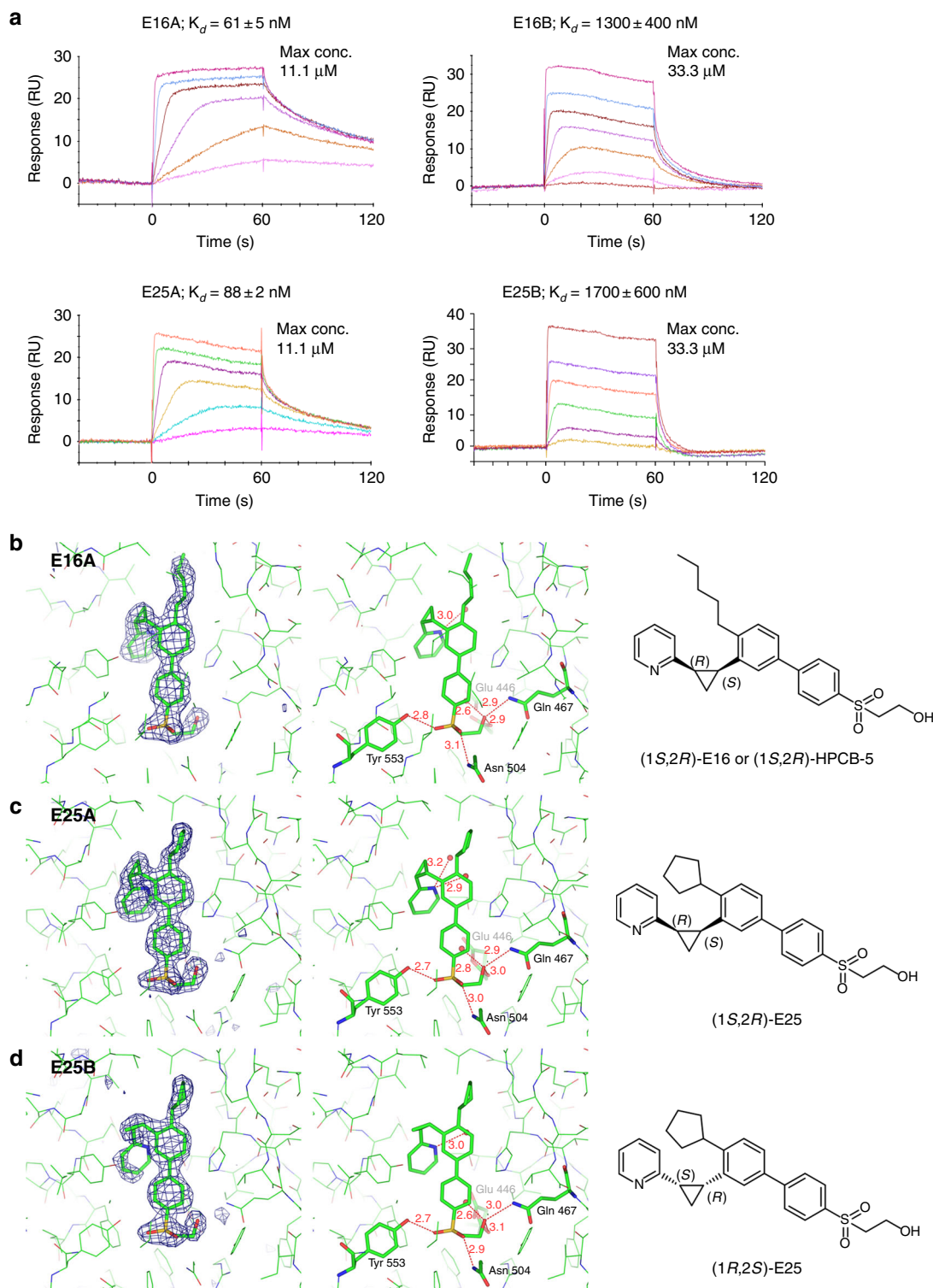


**Fig. 5** An optimized CERT inhibitor with a specific stereochemistry. After stereochemical separation of the racemic compounds E16 and E25, four purified compounds, E16A, E16B, E25A, and E25B, were obtained. **a** SPR sensorgrams of the immobilized CERT START domain at various concentrations of the four compounds as the analytes are shown. E16A and E25A showed higher affinity than their counterparts E16B and E25B. Co-crystallography of E16A or (1*S*, 2*R*)-HPCB-5 (**b**), E25A (**c**), and E25B (**d**) in complex with the CERT START domain was also performed. Red dashed lines: hydrogen bonds (distances are indicated in angstroms). According to the co-crystallography, the stereochemical structures of the compounds are depicted in the right part of the panels. In the co-crystals, E16A, E25B, and E25B are captured interacting with almost the identical protein conformation, forming hydrogen-bonding networks with specific amino acid residues (glutamic acid 446, glutamine 467, asparagine 504, and tyrosine 553) and hydrophobic interactions with the inner surface of the ceramide-binding pocket in the CERT START. Notably, the distal pyridine ring of E25B, not E25A, is disordered in the complex, which may support the lower affinity of E25B

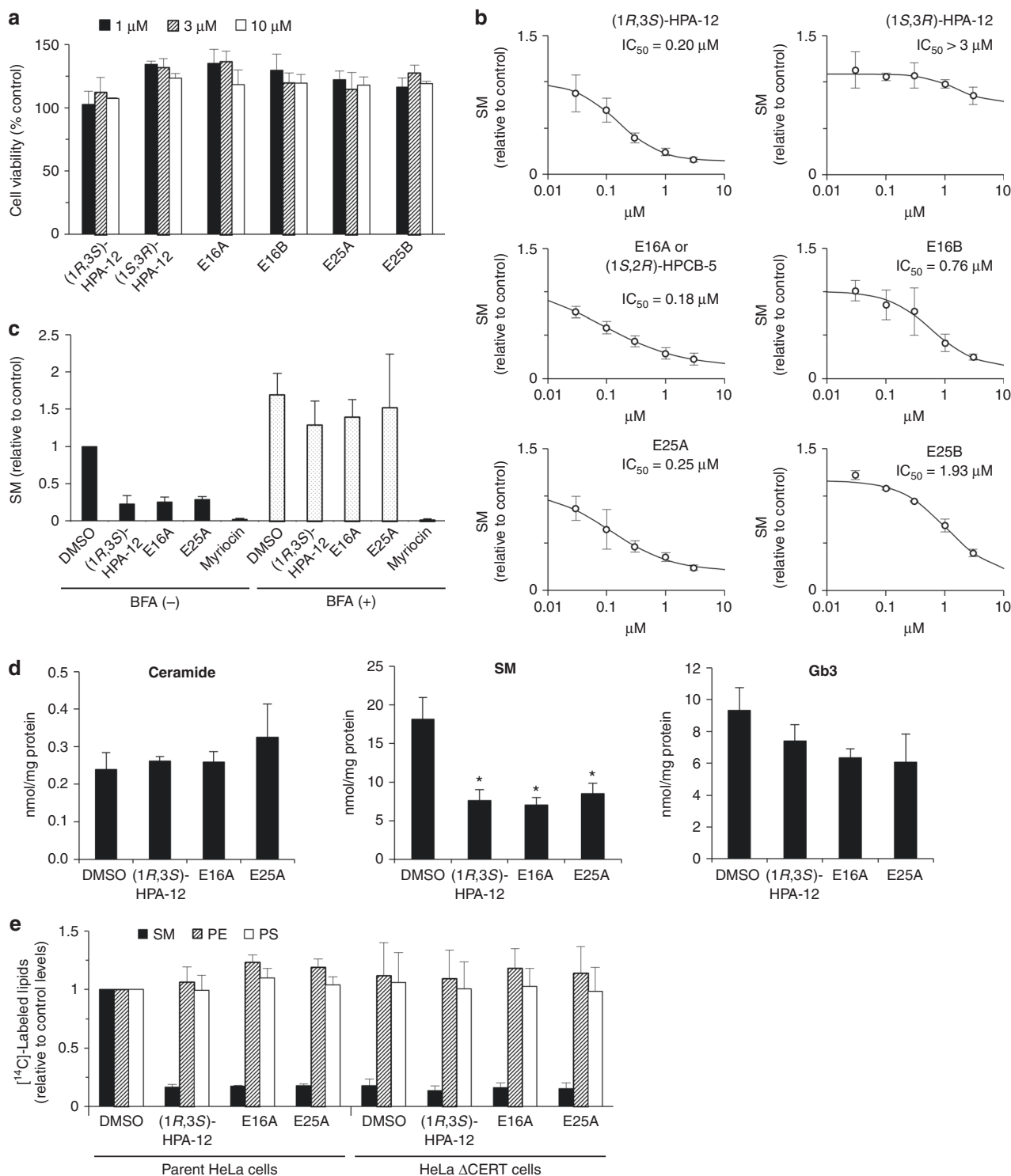


**Fig. 6** Potent inhibitors of CERT. **a** Cytotoxicity. After culture in normal culture medium in the presence or absence of the compounds at various concentrations for 24 h, the viability of the HeLa cells was assayed. The mean values  $\pm$  SD from three experiments are shown. **b** Inhibition of CERT in HeLa cells. The  $IC_{50}$  values for the metabolic labeling of SM were estimated from the dose-response curves. The mean values  $\pm$  SD from three experiments are shown. **c** Effect of BFA. After pre-incubation with BFA, HeLa cells were cultured with the compounds (3  $\mu M$  or the vehicle DMSO only) and L- $^{14}C$ serine for 8 h. The mean values  $\pm$  SD from three experiments are shown as the relative values of the vehicle control. **d** Effects of CERT inhibitors on the lipidome in cells. HeLa cells were cultured with the compounds (3  $\mu M$  or DMSO only) for 3 days in a serum-free medium. Then the various types of lipids in the cells were quantified by LC-MS. The mean values  $\pm$  SD from three experiments are shown. \* $P < 0.05$ . Gb3, trisaccharide globo-series sphingolipid. **e** CERT inhibitors do not affect CERT-independent synthesis of SM. A CERT-disrupted HeLa mutant and its parent cell lines were cultured with L- $^{14}C$ serine and the compounds (3  $\mu M$  or DMSO only) for 24 h. The mean values  $\pm$  SD from three experiments are shown as the relative values of the vehicle controls



chirality at the linker moiety between the pyridinyl and phenyl groups is advantageous for scaling up its chemical synthesis. Thus, we hereafter referred to B16 as HPEB-5 after its chemical name: 4'-(2-hydroxyethanesulfonyl)-4-pentyl-3-(pyridin-2-ylethyl)-1,1'-biphenyl).

## Discussion

The availability of LTP inhibitors remains very limited except for a few LTP types, including sterol or oxysterol transfer proteins<sup>27–30</sup> and CERT<sup>13,14,17,19</sup>. (1*R*, 3*S*)-HPA-12 and its closely related compounds have so far been the only potent inhibitors of CERT effective in living cells<sup>13,14,17,26,31</sup>. Iminosugar-based structures were recently shown to be another type of ceramide-mimicking CERT inhibitor, although their effectiveness toward living cells remains unclear<sup>19</sup>. In the present study, we developed (1*S*, 2*R*)-HPCB-5 as a novel potent CERT inhibitor with no apparent structural similarity to ceramides. To achieve this, there were several key experimental steps. First, virtual screening enabled us to screen millions of known compounds and identify a seed compound in a few months. This was owing to the previously resolved 3D structure of START, the ceramide-binding domain of CERT, in complex with natural ceramides<sup>12</sup> and ceramide-mimetic inhibitors<sup>13,14,17</sup>. Second, the determination that the azole group of the initial seed compound could be replaced with simpler structures without detrimental effects on the affinity toward the START domain lead us to rational synthetic routes to obtain a variety of seed derivatives using combinatorial chemistry. One-pot tandem reactions also facilitated the chemical synthesis of the A-series compounds. Third, the SPR-based assay system was useful to determine the absolute  $K_d$  values of chemical compounds for the START domain, thereby enabling us to efficiently select superior candidates among the virtually screened primary candidates. Fourth, there were reliable assay systems to evaluate the activity of the compounds to inhibit the function of CERT in living cells by employing various tools (e.g., BFA and CERT KO mutant HeLa cell lines) useful to assess the off-target effects of the selected compounds. Using these multidisciplinary approaches in concert, we identified a series of novel ceramide-unrelated compounds that potently inhibited the function of CERT in human cultured cells. The overall strategy may be applicable to other LTPs for the development of natural ligand-nonmimetic inhibitors.

Polar groups in a ceramide molecule are limited to only the 1-hydroxyl, 3-hydroxyl, and 2-amido groups (Fig. 1a). All three of these polar groups form a hydrogen-bonding network with specific amino acid residues in the CERT START domain, while van der Waals interactions between the hydrophobic moiety of ceramide and the inner surface of the ceramide-binding pocket in the START domain are also crucial for the recognition of ceramide by CERT<sup>12</sup>. HPA-12 is recognized by the CERT START domain in a similar manner<sup>17</sup>. (1*S*, 2*R*)-HPCB-5 shares two common features necessary for the high-affinity recognition by the CERT START domain. The hydroxyethanesulfonyl group in HPCB-5 forms hydrogen-bonding networks with specific amino acids in the START domain similar to ceramide (Fig. 5 and Supplementary Fig. 2). Moreover, the three aryl groups and *n*-pentyl groups of HPCB-5 with an appropriate conformation allow the compound to sufficiently occupy the hydrophobic pocket of the START domain (Fig. 5). Presumably, these are the most crucial structural features responsible for the ability of HPCB-5 with no ceramide-like structure to inhibit CERT with a similar degree of potency as the partial ceramide mimicry HPA-12. It should also be noted that enhancing the affinity of the lipid ligands for their cytoplasmic binding proteins by increasing their hydrophobicity often results in decreases in their water miscibility

and plasma membrane permeability, making them less effective toward living cells. In terms of the compounds developed in the present study, the  $K_d$  values determined by the cell-free SPR assay were well correlated to their potency levels for inhibiting CERT in living HeLa cells (Figs. 2, 4b), implying that the polar and membrane-permeable nature of the compounds also contributes to the ability of HPCB-5 to act as a potent CERT inhibitor in living cells.

Beyond its primary function to deliver ceramide from the ER to the Golgi apparatus, CERT participates in various biological events, including polyploid cancer cell death<sup>32</sup>, EGF receptor signaling<sup>33</sup>, lipotoxicity and glucolipotoxicity in islet  $\beta$ -cells<sup>34,35</sup>, muscle insulin signaling<sup>36</sup>, stress-induced Golgi disassembly<sup>37</sup>, protein secretions<sup>38</sup>, phosphoinositide turnover at the *trans* Golgi network<sup>39</sup>, cytotoxic autophagy<sup>40</sup>, and senescence<sup>41</sup>. Additionally, pharmacological or genetic inhibition of CERT negatively affects the proliferation of several types of intracellular pathogens<sup>42–46</sup>. Moreover, a point mutation causing the loss of repressive phosphorylation in the human CERT gene results in a hereditary mental development disorder with an autosomal dominant inheritance<sup>11</sup>. CERT inhibitors may serve as pharmaceutical seed compounds to prevent or ameliorate human diseases. A recent study suggested that a fluorinated derivative of HPA-12 can serve as an *in vivo* probe of CERT in positron emission tomography (PET) imaging<sup>26</sup>. A fluorinated HPCB-5 may also serve as a PET probe of CERT. Moreover, CERT and/or its longer splicing isoform CERT<sub>L</sub> (or Goodpasture antigen-binding protein), both of which have the intact ceramide-transfer START domain<sup>6</sup>, were demonstrated to bind various extracellular proteins, including type IV collagen<sup>47,48</sup>, serum amyloid P-component<sup>49</sup>, and the complement factor C1q<sup>50</sup>. New CERT inhibitors may also be a useful tool to investigate the pathophysiological meaning of interactions between CERT/CERT<sub>L</sub> and extracellular proteins, although it remains elusive whether the proposed extracellular functions of CERT/CERT<sub>L</sub> are relevant to its ceramide-transfer activity. Additionally, (1*R*, 3*S*)-HPA-12 and (1*S*, 2*R*)-HPCB-5 (and/or HPEB-5) together may provide a robust tool to discriminate on-target effects from off-target effects when CERT is pharmacologically inhibited as the same pathophysiological consequences induced by a pair of structurally dissimilar inhibitors are attributable directly or indirectly to the inhibition of CERT, not to off-target effects.

## Methods

**Materials and synthetic procedures.** See Supplementary Methods and Supplementary Figures 10–33.

**Virtual screening of a seed compound.** See Supplementary Methods.

**Purification of the CERT START domain.** See Supplementary Methods.

**SPR experiments.** See Supplementary Methods and Supplementary Figures 1–2.

**Protein crystallization.** See Supplementary Methods.

**Diffraction data collection and structure determination.** See Supplementary Methods, Supplementary Figures 3–4, and Supplementary Table 1.

**Bioassays within cell culture.** See Supplementary Methods, Supplementary Figures 5–7.

**Stability of CERT inhibitors.** See Supplementary Figures 8–9.

## Data availability

Crystallographic data have been deposited in the PDB with identifiers (6J0O, 5ZYG, 5ZYH, 6J81, 5ZYI, 5ZYK, 5ZYJ, 5ZYL, 5ZYM, 6IEZ, and 6IF0). Raw data (including <sup>1</sup>H- and <sup>13</sup>C-NMR charts of synthesized compounds) obtained in this study are available

from the generalist repository figshare (<https://doi.org/10.6084/m9.figshare.7398533>) or from the author upon reasonable request.

Received: 6 September 2018 Accepted: 23 January 2019

Published online: 20 February 2019

## References

- Hanada, K. Lipid transfer proteins rectify inter-organelle flux and accurately deliver lipids at membrane contact sites. *J. Lipid Res.* **59**, 1341–1366 (2018).
- Holthuis, J. C. & Menon, A. K. Lipid landscapes and pipelines in membrane homeostasis. *Nature* **510**, 48–57 (2014).
- Wong, L. H., Copic, A. & Levine, T. P. Advances on the transfer of lipids by lipid transfer proteins. *Trends Biochem. Sci.* **42**, 516–530 (2017).
- Goto, A., Charman, M. & Ridgway, N. D. Oxysterol-binding protein activation at endoplasmic reticulum-Golgi contact sites reorganizes phosphatidylinositol 4-phosphate pools. *J. Biol. Chem.* **291**, 1336–1347 (2016).
- Wang, P. Y., Weng, J. & Anderson, R. G. OSBP is a cholesterol-regulated scaffolding protein in control of ERK 1/2 activation. *Science* **307**, 1472–1476 (2005).
- Hanada, K. et al. Molecular machinery for non-vesicular trafficking of ceramide. *Nature* **426**, 803–809 (2003).
- Hanada, K. Co-evolution of sphingomyelin and the ceramide transport protein CERT. *Biochim. Biophys. Acta* **1841**, 704–719 (2014).
- Rao, R. P. et al. Ceramide transfer protein function is essential for normal oxidative stress response and lifespan. *Proc. Natl. Acad. Sci. USA* **104**, 11364–11369 (2007).
- Granero-Molto, F. et al. Goodpasture antigen-binding protein and its spliced variant, ceramide transfer protein, have different functions in the modulation of apoptosis during zebrafish development. *J. Biol. Chem.* **283**, 20495–20504 (2008).
- Wang, X. et al. Mitochondrial degeneration and not apoptosis is the primary cause of embryonic lethality in ceramide transfer protein mutant mice. *J. Cell Biol.* **184**, 143–158 (2009).
- Deciphering Developmental Disorders, S. Large-scale discovery of novel genetic causes of developmental disorders. *Nature* **519**, 223–228 (2015).
- Kudo, N. et al. Structural basis for specific lipid recognition by CERT responsible for nonvesicular trafficking of ceramide. *Proc. Natl. Acad. Sci. USA* **105**, 488–493 (2008).
- Yasuda, S. et al. A novel inhibitor of ceramide trafficking from the endoplasmic reticulum to the site of sphingomyelin synthesis. *J. Biol. Chem.* **276**, 43994–44002 (2001).
- Kumagai, K. et al. CERT mediates intermembrane transfer of various molecular species of ceramides. *J. Biol. Chem.* **280**, 6488–6495 (2005).
- Duris, A. et al. Expedient and practical synthesis of CERT-dependent ceramide trafficking inhibitor HPA-12 and its analogues. *Org. Lett.* **13**, 1642–1645 (2011).
- Ueno, M., Huang, Y. Y., Yamano, A. & Kobayashi, S. Revised stereochemistry of ceramide-trafficking inhibitor HPA-12 by X-ray crystallography analysis. *Org. Lett.* **15**, 2869–2871 (2013).
- Kudo, N. et al. Crystal structures of the CERT START domain with inhibitors provide insights into the mechanism of ceramide transfer. *J. Mol. Biol.* **396**, 245–251 (2010).
- Santos, C. et al. Identification of novel CERT ligands as potential ceramide trafficking inhibitors. *Chembiochem* **15**, 2522–2528 (2014).
- Santos, C. et al. Iminosugar-based ceramide mimicry for the design of new CERT START domain ligands. *Bioorg. Med. Chem.* **25**, 1984–1989 (2017).
- Duris, A. et al. Asymmetric synthesis and binding study of new long-chain HPA-12 Analogues as potent ligands of the ceramide transfer protein CERT. *Chem. Eur. J.* **22**, 6676–6686 (2016).
- Santos, C. et al. The CERT antagonist HPA-12: first practical synthesis and individual binding evaluation of the four stereoisomers. *Bioorg. Med. Chem.* **23**, 2004–2009 (2015).
- Fukasawa, M., Nishijima, M. & Hanada, K. Genetic evidence for ATP-dependent endoplasmic reticulum-to-Golgi apparatus trafficking of ceramide for sphingomyelin synthesis in Chinese hamster ovary cells. *J. Cell Biol.* **144**, 673–685 (1999).
- Hanada, K. Serine palmitoyltransferase, a key enzyme of sphingolipid metabolism. *Biochim. Biophys. Acta* **1632**, 16–30 (2003).
- Hanada, K. et al. Sphingolipids are essential for the growth of Chinese hamster ovary cells. Restoration of the growth of a mutant defective in sphingoid base biosynthesis by exogenous sphingolipids. *J. Biol. Chem.* **267**, 23527–23533 (1992).
- Yamaji, T. & Hanada, K. Establishment of HeLa cell mutants deficient in sphingolipid-related genes using TALENs. *PLoS ONE* **9**, e88124 (2014).
- Crivelli, S. M. et al. Synthesis, radiosynthesis, and preliminary in vitro and in vivo evaluation of the fluorinated ceramide trafficking inhibitor (HPA-12) for brain applications. *J. Alzheimers Dis.* **60**, 783–794 (2017).
- Akula, N., Midzak, A., Lecanu, L. & Papadopoulos, V. Identification of small-molecule inhibitors of the steroidogenic acute regulatory protein (STAR1) by structure-based design. *Bioorg. Med. Chem. Lett.* **22**, 4139–4143 (2012).
- Burgett, A. W. et al. Natural products reveal cancer cell dependence on oxysterol-binding proteins. *Nat. Chem. Biol.* **7**, 639–647 (2011).
- Arita, M. et al. Oxysterol-binding protein family I is the target of minor enviroxime-like compounds. *J. Virol.* **87**, 4252–4260 (2013).
- Strating, J. R. et al. Itraconazole inhibits enterovirus replication by targeting the oxysterol-binding protein. *Cell Rep.* **10**, 600–615 (2015).
- Nakamura, Y. et al. Stereoselective synthesis and structure-activity relationship of novel ceramide trafficking inhibitors. (1R,3R)-N-(3-hydroxy-1-hydroxymethyl-3-phenylpropyl)dodecanamide and its analogues. *J. Med. Chem.* **46**, 3688–3695 (2003).
- Swanton, C. et al. Regulators of mitotic arrest and ceramide metabolism are determinants of sensitivity to paclitaxel and other chemotherapeutic drugs. *Cancer Cell* **11**, 498–512 (2007).
- Heering, J. et al. Loss of the ceramide transfer protein augments EGF receptor signaling in breast cancer. *Cancer Res.* **72**, 2855–2866 (2012).
- Guo, J. et al. Palmitate-induced inhibition of insulin gene expression in rat islet beta-cells involves the ceramide transport protein. *Cell Physiol. Biochem.* **26**, 717–728 (2010).
- Gjoni, E. et al. Glucolipotoxicity impairs ceramide flow from the endoplasmic reticulum to the Golgi apparatus in INS-1 beta-cells. *PLoS ONE* **9**, e110875 (2014).
- Bandet, C. L. et al. Ceramide transporter CERT is involved in muscle insulin signaling defects under lipotoxic conditions. *Diabetes* **67**, 1258–1271 (2018).
- Chandran, S. & Machamer, C. E. Inactivation of ceramide transfer protein during pro-apoptotic stress by Golgi disassembly and caspase cleavage. *Biochem. J.* **442**, 391–401 (2012).
- Fugmann, T. et al. Regulation of secretory transport by protein kinase D-mediated phosphorylation of the ceramide transfer protein. *J. Cell Biol.* **178**, 15–22 (2007).
- Capasso, S. et al. Sphingolipid metabolic flow controls phosphoinositide turnover at the trans-Golgi network. *EMBO J.* **36**, 1736–1754 (2017).
- Hernandez-Tiedra, S. et al. Dihydroceramide accumulation mediates cytotoxic autophagy of cancer cells via autolysosome destabilization. *Autophagy* **12**, 2213–2229 (2016).
- Rao, R. P. et al. Ceramide transfer protein deficiency compromises organelle function and leads to senescence in primary cells. *PLoS ONE* **9**, e92142 (2014).
- Aizaki, H. et al. Critical role of virion-associated cholesterol and sphingolipid in hepatitis C virus infection. *J. Virol.* **82**, 5715–5724 (2008).
- Amako, Y., Syed, G. H. & Siddiqui, A. Protein kinase D negatively regulates hepatitis C virus secretion through phosphorylation of oxysterol-binding protein and ceramide transfer protein. *J. Biol. Chem.* **286**, 11265–11274 (2011).
- Otsuki, N. et al. Both sphingomyelin and cholesterol in the host cell membrane are essential for Rubella virus entry. *J. Virol.* **92**, e01130–17 (2017).
- Derre, I., Swiss, R. & Agaisse, H. The lipid transfer protein CERT interacts with the Chlamydia inclusion protein IncD and participates to ER-Chlamydia inclusion membrane contact sites. *PLoS Pathog.* **7**, e1002092 (2011).
- Elwell, C. A. et al. Chlamydia trachomatis co-opts GBF1 and CERT to acquire host sphingomyelin for distinct roles during intracellular development. *PLoS Pathog.* **7**, e1002198 (2011).
- Raya, A., Revert, F., Navarro, S. & Saus, J. Characterization of a novel type of serine/threonine kinase that specifically phosphorylates the human goodpasture antigen. *J. Biol. Chem.* **274**, 12642–12649 (1999).
- Raya, A. et al. Goodpasture antigen-binding protein, the kinase that phosphorylates the goodpasture antigen, is an alternatively spliced variant implicated in autoimmune pathogenesis. *J. Biol. Chem.* **275**, 40392–40399 (2000).
- Mencarelli, C. et al. Goodpasture antigen-binding protein/ceramide transporter binds to human serum amyloid P-component and is present in brain amyloid plaques. *J. Biol. Chem.* **287**, 14897–14911 (2012).
- Bode, G. H. et al. Complement activation by ceramide transporter proteins. *J. Immunol.* **192**, 1154–1161 (2014).

## Acknowledgements

We thank Dr. Kouichi Uoto (Daiichi Sankyo Co., Ltd., Tokyo, Japan) for his gifts of newly synthesized HPA-12 compounds, and Dr. Toshiyuki Yamaji (Department of Biochemistry and Cell Biology, National Institute of Infectious Diseases, Tokyo, Japan) for his support of in-house quality tests of cultured cells. We thank Drs. Noriyuki Igarashi and Naohiro Matsugaki for their help with the data collection at beam line NW12A of the Photon factory advanced ring (PF-AR), and Dr. Renee Mosi from Edanz Group ([www.edanzediting.com/ac](http://www.edanzediting.com/ac)) for editing a draft of this manuscript. This work was

supported in part by MEXT for Scientific Research on Innovative Area (KAKENHI grant number: 17H06417 to K.H.), by Japan AMED for AMED-CREST (JP18gm0910005j0004 to K.H.), and by a collaboration research grant from Daiichi Sankyo Co., Ltd. (to S.K.).

### Author contributions

Overall planning: S.K. and K.H.; design and performing experiments: N.N., M.U., S.S., D. E., H.H., S.K., K.K. and M.S.; data analysis: N.N., M.U., S.S., D.E., H.H., S.K., K.K., M.S., S.K. and K.H.; paper writing: N.N., M.U., S.S., D.E., H.H., S.K. and K.H. All authors read and approved the paper.

### Additional information

**Supplementary information** accompanies this paper at <https://doi.org/10.1038/s42004-019-0118-3>.

**Competing interests:** The authors declare no competing interests.

**Reprints and permission** information is available online at <http://npg.nature.com/reprintsandpermissions/>

**Publisher's note:** Springer Nature remains neutral with regard to jurisdictional claims in published maps and institutional affiliations.



**Open Access** This article is licensed under a Creative Commons Attribution 4.0 International License, which permits use, sharing, adaptation, distribution and reproduction in any medium or format, as long as you give appropriate credit to the original author(s) and the source, provide a link to the Creative Commons license, and indicate if changes were made. The images or other third party material in this article are included in the article's Creative Commons license, unless indicated otherwise in a credit line to the material. If material is not included in the article's Creative Commons license and your intended use is not permitted by statutory regulation or exceeds the permitted use, you will need to obtain permission directly from the copyright holder. To view a copy of this license, visit <http://creativecommons.org/licenses/by/4.0/>.

© The Author(s) 2019